

# Lattice trapping and crack decohesion in graphene



Fanchao Meng, Cheng Chen, Jun Song\*

Department of Mining and Materials Engineering, McGill University, Montréal, Québec, H3A 0C5, Canada

## ARTICLE INFO

### Article history:

Received 25 September 2016

Received in revised form

5 January 2017

Accepted 27 January 2017

Available online 31 January 2017

## ABSTRACT

Lattice trapping is an important aspect in accurately understanding the fracture behaviors of nano-materials. Employing molecular dynamics simulations, we studied the lattice trapping of nanocracks in both single-crystal and polycrystalline graphene. Different crack-dislocation and crack-grain boundary configurations were constructed and investigated. It is found that cracks in single-crystal graphene exhibit negligible lattice trapping, with or without the presence of dislocations. On the other hand, lattice trapping in polycrystalline graphene may vary greatly and is shown to be directly correlated to the tensile strength of grain boundary. Moreover, we showed that unique dislocation-independent traction-separation behaviors, which are not affected by the presence of dislocations, exist for cracks in single-crystal graphene. The traction-separation relation was then fitted to a cohesive zone model to demonstrate the possibility of bridging atomistic modeling with large-scale numerical simulations. Our findings provide critical hints for atomistic-informed multiscale modeling of fracture of two-dimensional materials.

© 2017 Elsevier Ltd. All rights reserved.

## 1. Introduction

Owing to its two-dimensional (2D) crystal structure and exceptional physical properties, graphene opens the horizon for new physics explorations and promises numerous next-generation applications [1–6]. In particular, its extraordinary mechanical properties, e.g., a Young's modulus of ~1 TPa and an intrinsic fracture strength of ~130 GPa [7], nominate graphene as the prospective building material in nanodevices such as graphene-supplemented nanocomposites [8,9], 2D impermeable atomic-scale pressure barriers [10,11], and size-selective molecular separation membranes [12,13], where high material stiffness and strength are central to device stability and durability. Yet it has been demonstrated by many studies that the existence of topological defects, such as dislocations and grain boundaries (GBs) [14], which often arise during its large-scale fabrications [15], can greatly alter the strength of graphene, causing premature fracture failures [16–18]. This thus posts a serious concern for the mechanical robustness of graphene-based devices. For example, it has been experimentally shown that the fracture load of a chemical vapor deposition fabricated polycrystalline graphene is one order of magnitude lower than that of exfoliated single-crystal graphene

[15,19], and theoretically demonstrated that graphene with low angle GBs can lose more than 50% of its strength [17,20,21].

Despite that a large amount of work toward understanding the effects of topological defects on fracture behaviors of graphene was reported [15,17,19–21], an important aspect often overlooked is the lattice trapping/arrestment of cracks [22] in graphene. To date, though there have been some studies on lattice trapping for pristine single-crystal graphene [16,23], it remains elusive how lattice trapping may change in the presence of topological defects since lattice trapping strongly depends on atomic details at the crack tip and the forces required to break bonds successively [24,25].

In this study, we examined lattice trapping of nanocracks in single-crystal and polycrystalline graphene using large-scale molecular dynamics (MD) simulations. The effects of dislocations and grain boundaries on lattice trapping are clarified. Our results indicated that for a crack in single-crystal graphene, there exists a unique traction-separation relationship which remains unaltered in the presence of dislocations. The traction-separation relation was then interpreted within the framework of cohesive zone model (CZM), to demonstrate the possible route to translate atomistic information to large-scale numerical simulations of fracture of graphene.

## 2. Computational method

To study the roles of dislocations or GBs in lattice trapping of graphene, several crack-dislocation and crack-GB configurations

\* Corresponding author.

E-mail address: [jun.song2@mcgill.ca](mailto:jun.song2@mcgill.ca) (J. Song).

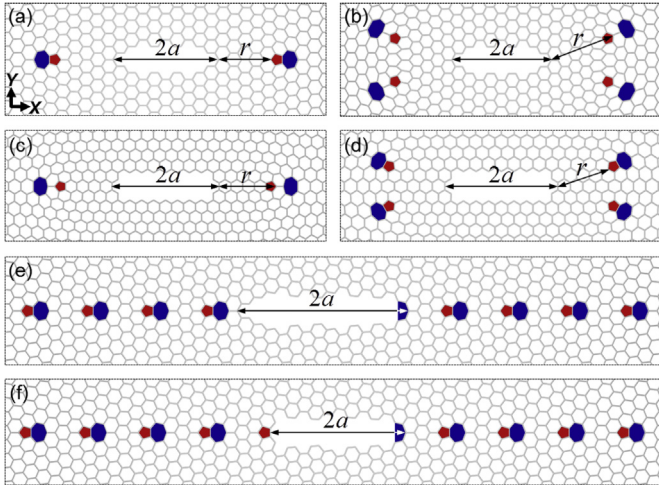


**Fig. 1.** Sample crack-dislocation configurations, i.e., an armchair crack accompanied by an (a) (1,0) dislocation pair  $[AC|(1,0)_P]$  and (b) (1,1) dislocation quartet  $[AC|(1,1)_Q]$ , and a zigzag crack accompanied by an (c) (1,1) dislocation pair  $[ZZ|(1,1)_P]$  and (d) (1,0) dislocation quartet  $[ZZ|(1,0)_Q]$ , along with representative crack-GB configurations with the crack sitting along the  $\Sigma 19$  ( $\theta = 13.2^\circ$ ) GB, i.e., cracks consisting of (e) armchair-like and heptagon crack tips (AC/HP) and (f) pentagon and heptagon crack tips (PN/HP), respectively. The internal crack has a crack size of  $2a$  and the separation between crack and dislocation is measured from the crack tip to the pentagon tip of the dislocation and is denoted as  $r$ . Dash lines indicate the simulation supercells are fully periodic along the in-plane directions. (A colour version of this figure can be viewed online.)

were constructed, as illustrated in Fig. 1. The crack-dislocation configuration comprises either an armchair (AC) or a zigzag (ZZ) internal crack along with two or four dislocations distributed symmetrically on both sides of the crack. The following dislocation configurations, being (1,0) pair (Fig. 1a) and (1,1) quartet (Fig. 1b) for AC cracks, and (1,1) pair (Fig. 1c) and (1,0) quartet (Fig. 1d) for ZZ cracks, were considered in our study, where the notations (1,0) and (1,1) represent edge dislocations of Burger's vectors  $|\vec{b}_{(1,0)}| = a_0$  and  $|\vec{b}_{(1,1)}| = \sqrt{3}a_0$ , respectively, with  $a_0 = 2.42$  Å being the lattice constant of the pristine graphene [26–28]. For simplicity, the above crack-dislocation configurations are denoted as  $AC|(1,0)_P$ ,  $AC|(1,1)_Q$ ,  $ZZ|(1,1)_P$  and  $ZZ|(1,0)_Q$ , respectively. For crack-GB configurations, several symmetric tilt GBs (STGBs), with respective misorientation angle  $\theta$  being  $9.5^\circ$ ,  $13.2^\circ$ ,  $16.4^\circ$ , and  $21.8^\circ$ , were considered. The dislocation was constructed by inserting a semi-infinite strip of carbon atoms into the otherwise perfect graphene lattice [14,29], while the GB was constructed by rotating two separate graphene lattices and then stitching them together [21,30] (see Supplementary Data S1 for details). The crack resides directly along the GB and was created by removing a thin strip of atoms. Depending on the way atoms are removed, there can be two types of cracks of different crack tip configurations. As illustrated in Fig. 1e–f using the  $\Sigma 19$  ( $\theta = 13.2^\circ$ ) STGB as the representative system (See Supplementary Data S2 for figures of the other STGBs), one crack type consists of AC-like and heptagon crack tips (see Fig. 1e), while the other consists of pentagon and heptagon crack tips (see Fig. 1f). In the following context, we refer to these two types of cracks as AC/HP and PN/HP, respectively. One important thing to note is that it is necessary to include the heptagon crack tip when constructing a crack along an STGB because otherwise fracture would first occur away from the crack tip at a bond shared by heptagon and hexagon due to the presence of high prestresses in such bonds [20,31].

Periodic boundary conditions are used in our simulations and the in-plane shape of the supercell is rectangular with width and height in 600–800 Å and 700–1000 Å for crack-dislocation

configuration depending on the detailed type and number of dislocations (note that benchmark calculations were performed to ensure ignorable size dependence due to dislocation/crack interactions across the periodic boundaries), and 600 Å and 1000 Å for crack-GB configuration, respectively. In addition, the distance between dislocations on the symmetric side of the internal crack remains  $\sim 150$  Å for all crack-dislocation configurations. The interlayer distance is set as 15 Å to avoid interlayer interactions in the direction perpendicular to the graphene sheet. Meanwhile, the lattice trapping of the dislocation- and GB-free supercells were also examined as a reference state.

Large-scale MD simulations using LAMMPS package [32] are employed to investigate the lattice trapping in graphene with topological defects. The widely used adaptive intermolecular reactive empirical bond order (AIREBO) potential [33] is adopted to simulate mechanical behaviors of graphene [34–37], where the original cut-off radius (1.7 Å) of the first nearest neighboring distance of hydrocarbons has been modified to 2.0 Å to avoid the non-physical post-hardening behavior in simulating stress-strain response of graphene [34–37]. Before loading on the supercell, a relaxation period of 100 ps was performed to attain zero normal pressures along the in-plane directions (i.e.,  $P_{XX} = P_{YY} = 0$ , see Fig. 1) using NPT ensemble [38,39], following which the system was deformed by an in-plane uniaxial tension with a strain rate of  $0.001 \text{ ps}^{-1}$  along  $Y$  direction (i.e., the in-plane direction perpendicular to the crack, see Fig. 1) to drive crack propagation. Note that the out-of-plane deformation of the 2D graphene is suppressed during the simulation because lattice trapping and CZM law are not well defined for a 2D sheet buckled in the thickness direction, although our preliminary study showed the out-of-plane deformation exerts a negligible effect on the in-plane results reported here (see Supplementary Data S3 for details). The timestep was set as 1 fs while a constant temperature of  $T = 1$  K was maintained for all simulations. Though in the present study we are using a specific strain rate ( $0.001 \text{ ps}^{-1}$ ) and temperature ( $T = 1$  K), additional calculations with lower strain rates (as low as  $10^{-5} \text{ ps}^{-1}$ ) and higher temperatures (up to  $T = 300$  K) have been performed to confirm that our results are not strain rate and temperature dependent (see Supplementary Data S4 for details).

### 3. Results and discussion

#### 3.1. Determination of lattice trapping using $J$ -integral

The degree of lattice trapping ( $\lambda_{LP}$ ) in graphene with or without defects is defined as the ratio of strain energy release rate to fracture energy. In light of certain nonlinearity in the stress-strain response of graphene [23], strain energy release rate is quantified by calculating the critical value of  $J$ -integral ( $J_c$ ) [40] at crack growth using the equivalent domain integral (EDI) method [41]. The fracture energy  $\Gamma$  is defined as

$$\Gamma = 2\gamma \quad (1)$$

where  $\gamma$  is the surface energy density that can be calculated from the energy difference per unit area between pristine graphene and graphene with two newly created surfaces (see Supplementary Data S5 for details). Thus, we have

$$\lambda_{LP} = J_c / 2\gamma \quad (2)$$

Apparently, in the absence of lattice trapping, we have  $\lambda_{LP} = 1$ .

The domain integral (see domain  $S$  illustrated in Fig. 2) used to calculate  $J$ -integral is given by

Download English Version:

<https://daneshyari.com/en/article/5432155>

Download Persian Version:

<https://daneshyari.com/article/5432155>

[Daneshyari.com](https://daneshyari.com)